Fire Safety Journal 141 (2023) 103909

Contents lists available at ScienceDirect

Fire Safety Journal

journal homepage: www.elsevier.com/locate/firesaf

The analysis of traffic data of wildfire evacuation: the case study of the 2020 Glass Fire

Arthur Rohaert [a], Nima Janfeshanaraghi [b], Erica Kuligowski [b], Enrico Ronchi [a,*]

[a] Division of Fire Safety Engineering, Lund University, Lund, Sweden
[b] RMIT University, Melbourne, Victoria, Australia

ARTICLE INFO

Keywords:
Evacuation
Wildfire
Traffic dynamics
Wildland-urban interface
Modelling
Glass Fire

ABSTRACT

Evacuation is a crucial policy to mitigate wildfire impacts. Understanding traffic dynamics during a wildfire evacuation can help authorities to improve in improving emergency management plans, thus improving life safety. In this study, we developed a methodology to extract historical traffic data from vehicle detector stations and automate the analysis of traffic dynamics for actual wildfire evacuations. This has been implemented in an open-access tool called Traffic Dynamic Analyser (TDA) which generates speed-density and flow-density relationships from data using both commonly used macroscopic traffic models as well as machine learning techniques (e.g., support vector regression). The use of the methodology is demonstrated with a case study of the 2020 Glass Fire in California, USA. The results from TDA showed a slight reduction in speeds and flows on US Highway 101 during the evacuation scenario, compared with the routine scenario. Moreover, background traffic has been shown to play a key role in the 2020 Glass Fire compared with previous wildfire evacuation scenarios (e.g., the 2019 Kincade fire). The case study showed that the methodology implemented in the TDA can be used to understand traffic evacuation dynamics in wildfire scenarios and to validate evacuation models.

1. Introduction

Climate change and other anthropogenic factors (such as forest management and suppression policies) have led to longer wildfire seasons worldwide and increased fire frequency and intensity during these seasons [1]. Moreover, the wildland-urban interface (WUI) has also increased [2]. Improved evacuation planning and real-time decision-making are essential to minimise the negative impacts of these trends on communities.

Wildfire evacuation models have great potential to support evacuation planning and real-time decision-making and traffic management. To provide an accurate estimation of the evacuation process, these models should consider the different aspects of a wildfire event (i.e., fire and smoke spread, decision-making, pedestrian response and movement, and traffic), as well as the interaction between these aspects [3,4]. Ronchi et al. [4] assessed the potential of existing fire models, pedestrian models and traffic models to be used in a multi-layer evacuation simulation model for wildfires. Moreover, researchers have started to develop integrated models for wildfire evacuation [5–11]. Kuligowski [12] and Ronchi and Gwynne [13] argue that due to our currently limited understanding of evacuee decision-making processes and the lack of data to validate the model layers, further research efforts should focus on data collection and analysis.

Traffic models are one of the modelling layers that need further validation datasets. Many macroscopic, mesoscopic and microscopic traffic models could be used for wildfire evacuation modelling [14]. However, these models have been calibrated using data from non-evacuation scenarios. Calibration and validation efforts of these models for emergency scenarios are limited by a lack of data on evacuee travel behaviour and traffic dynamics during wildfire evacuations [9,12,15–17]. The importance of these data is highlighted by Dixit and Wolshon [18], who found a 10%–16% reduction in road capacity in USA hurricane evacuation events when compared with non-emergency traffic data. Factors identified as influential of this difference include unfamiliarity with the mode chosen, increased passenger load of the vehicle, increased vehicle length or change in desired headway (related to increased risk perception). Recent studies [19] on traffic dynamics during a wildfire event show similar trends. Analysis of traffic data collected both before and after the 2019 Kincade Fire in Sonoma County, California found that vehicle speeds during the fire event were reduced by approximately 3.5 km/h for densities between 0 and 64 veh/km/lane and the capacity was reduced by approximately 5% when compared with routine conditions. However, as this is one event, further research is needed to confirm these results for other fires.

* Corresponding author.
E-mail address: enrico.ronchi@brand.lth.se (E. Ronchi).

https://doi.org/10.1016/j.firesaf.2023.103909
Received 30 May 2023; Accepted 16 August 2023
Available online 2 September 2023

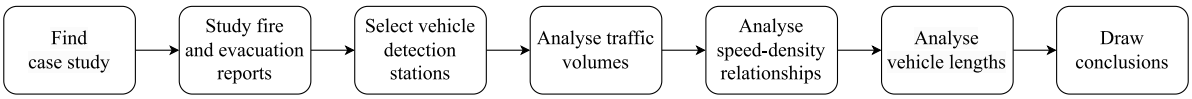

Fig. 1. Schematic presentation of the proposed methodology.

If results are consistent during other wildfire evacuations, they will need to be accounted for by traffic models to obtain realistic evacuation times. This means that the existing parameters of the speed-density and flow-density relationships (macroscopic modelling) or the car-following model (microscopic modelling) would require adjustments.

This paper presents a novel methodology for extracting and analysing data from traffic detectors for wildfire evacuation applications. While previous studies have recognised the need for data on traffic dynamics during wildfire evacuations, our work addresses this gap by providing a practical solution. The methodology has been developed and it has been implemented in a dedicated tool (including a graphical user interface) which is made freely available to all interested parties.

The aims of this work are (1) to demonstrate the functionalities of the methodology employed to obtain traffic evacuation datasets in wildfires from detector data, and (2) to provide open access to a dataset from an actual wildfire event used to show the use of the tool, the 2020 Glass Fire in California, USA.

2. Methodology

Our methodology is schematically summarised in Fig. 1. This section introduces some key modelling concepts needed to interpret the traffic dynamics. This is followed by an introduction to the traffic database we used and by the methodology proposed for data selection and model fitting. The paper focuses on macroscopic traffic modelling since these models can be calibrated and validated with data from traffic detector databases. Due to their lower computational requirements, they are deemed suitable for real-time wildfire evacuation applications.

2.1. Macroscopic traffic evacuation modelling

In macroscopic models, the traffic dynamics are generally described by three quantities: (1) the average vehicle speed v (km/h), (2) the traffic density k (veh/km/lane), (3) and the traffic flow q (veh/h/lane). These quantities are calculated for each road segment and for each time step by means of three relationships: the conservation of vehicles, the fundamental equation of traffic flow ($q = kv$), and the speed-density relationship (often referred to as 'macroscopic models' themselves).

The first speed-density relationship was proposed by Greenshields in 1935 [20]. Since then, many have followed. Well-known models include the exponential model, developed by Underwood [21], the North-Western model by Drake et al. [22], the bi-linear (triangular) model by Daganzo [23], the model by Van Aerde and Rakha [24,25], the model by Del Castillo and Benítez [26] and the model by Cheng et al. [27].

Traffic detection systems can generally measure speed, flow, and density. Therefore, it is possible to calibrate the parameters of macroscopic models by fitting the models onto traffic data and comparing the obtained values for routine scenarios with those of evacuation scenarios. Here, only the model by Daganzo [23] (Eq. (1)), the model by Van Aerde and Rakha [24,25] (Eq. (2)) and the model by Cheng et al. [27] (Eq. (3)) are presented, as these models are most frequently used today and fit best with the data of our case study. Details on the calibration of additional models are available in [28]. The first two models rely only on physical parameters: v_f (the free-flow speed); v_c (the critical speed), $q_c = k_c v_c$ (the critical flow, capacity), k_c (the critical density), and k_j (the jam density). The model by Cheng et al. [27] also relies on the polynomial order m.

$$v = \min\left(v_f, v_f \frac{\left(\frac{1}{k} - \frac{1}{k_j}\right)}{\left(\frac{1}{k_c} - \frac{1}{k_j}\right)}\right) \tag{1}$$

$$k = \frac{1}{a + \frac{b}{v_f - v} + cv} \text{ with } \begin{cases} a = \frac{v_f(2v_c - v_f)}{k_j v_c^2} \\ b = \frac{v_f(2v_c - v_f)^2}{k_j v_c^2} \\ c = \frac{1}{k_c v_c} - \frac{v_f}{k_j v_c^2} \end{cases} \tag{2}$$

$$v = \frac{v_f}{\left(1 + \left(k/k_c\right)^m\right)^{2/m}} \tag{3}$$

2.2. Caltrans PEMS database

As an example of a traffic database that can be used as a data source for wildfire evacuation studies, we adopted the Performance Measurement System (PeMS) of the California Department of Transportation (Caltrans). This database was established introduced in 1999, in cooperation with the University of California, Berkeley [29]. Today, it collects real-time traffic data from more than 46 600 detectors spread over more than 19 000 vehicle detection stations (VDSs) along the Californian freeway system. The data is stored and made available online (https://pems.dot.ca.gov/) and can be used to analyse traffic dynamics and service quality along major highways across the state. Moreover, the database contains incident records from the California Highway Patrol and lane closure records from Caltrans Headquarters [29].

The most common detector in PeMS is the loop detector (64% of VDSs are equipped with inductive loops). A loop detector is essentially a wire that is installed in a sealed loop-shaped saw cut, just beneath the road surface [30]. The wire acts like a coil. When a vehicle passes over the coil, it generates a vortex current in the loop such that the loop's inductance decreases by a few percent [30]. Consequently, one loop is able to detect the traffic flow and the detector occupancy. Some VDSs are equipped with dual loops, which consist of two loops, typically positioned three to four metres apart from each other [31]. These dual loops can also obtain the vehicle speed as the ratio of the loop distance and the detection delay ($v = \Delta x/\Delta t$).

While no specific studies could be identified determining the accuracy detectors used by Caltrans, other studies have demonstrated the high level of accuracy of inductive loops in general. Studies on similar loops in Minnesota show that the flow accuracy lies between 97.0 and 99.9% when comparing it with a manual count from video footage and that the speed accuracy lies between 96.7 and 98.8% when compared to the verified speedometer of a probe vehicle [32]. Research performed in Texas [30] reveals a mean error in vehicle speed of approximately 2.4 km/h (1.5 mph), in comparison to an infrared sensor speed trap.

Based on the studies mentioned above, traffic detector data can be considered among the most accurate data available to investigate traffic dynamics and was for this reason been chosen in this study.

2.3. Data selection

With the database identified, the next step is to select a dataset from PeMS for a specific wildfire event to understand traffic dynamics under emergency conditions and compare it with the traffic dynamics under routine conditions. This requires the identification of a set time frame

(e.g., before, during, and after the fire event) and specific freeways of interest (e.g., one or two freeways that are either directly within or adjacent to the evacuation zones). Once the time frame and location are set, the data selection process can begin. This process considers the following five aspects:

1. Detector position.
   Since the traffic dynamics on the mainline (i.e., the primary travel lanes of a highway) and ramps (junctions) are expected to differ, only the detector stations on the mainline of the highway are considered for this demonstration.
2. Speed measurement
   Not all detector stations measure the speed. For those that do not, PeMS employ an algorithm to estimate the speed from data from nearby stations (via the Daily Length Profile Algorithm by Erik van Zwet, [29]). To avoid noise and bias, only detector stations that measure the speed are considered.
3. Detector health
   The measurements of a detector station might be erroneous. The PeMS database automatically identifies unreliable data and calculates the health of the data (i.e., the percentage of reliable data) that is produced by the detector station. To avoid unreliable results, only detector stations with a health of 97% or more during the measurement campaigns, are considered.
4. Visual inspection
   The detector stations that meet the three conditions above are then subjected to a visual inspection. First, they are located on satellite images to ensure that all lanes belong to the mainline, and not to a junction or weaving zone. Second, graphs are produced that display the evolution of speed, flow, and density over time for each lane, as well as graphs that relate the speed, flow, and density. Only stations for which the graphs show physically credible results are considered.
5. Spacing
   Stations that are located close to each other will record correlated data because the same vehicles will be recorded, at almost the same moment. A selection is made to include as many stations as possible while maintaining a spacing of at least 2 km between the selected stations. This choice was a compromise between not discarding too much data and avoiding data being too correlated.

The flowchart in Fig. 4 summarises this process and the outcome related to the case study (see Section 4).

2.4. Data analysis

The methodology proposed here includes a dedicated procedure for model fitting which accounts for the peculiarities of the data under consideration. The macroscopic models $v = f(k)$ can be fitted to traffic data by minimising the sum of squares (S) of the residuals (error on the speed predictions). We used the Levenberg–Marquardt algorithm [33,34]. The residuals are weighted as proposed by Qu et al. [35] to ensure that the model fits well over the full range of densities (see Eq. (4) [35], where all m data points are ordered so that $k_i \leq k_j$ when $i < j$). Without weighting, the models would typically fit poorly in the high-density region due to the imbalance that is often observed in traffic data.

$$S = \sum_{i}^{m} w_i \left(v_i - f(k_i)\right)^2 \tag{4}$$

where

$$w_i = \begin{cases} (k_2 - k_1) & i = 1 \\ (k_{i+1} - k_{i-1})/2 & i = 2, 3, \ldots, m-1 \\ (k_m - k_{m-1}) & i = m \end{cases}$$

It is also possible to compare the trends of the evacuation data and routine data without assuming an underlying speed-density relationship. To do so, two machine learning methods are applied. The first method is Gaussian Kernel Smoothing (GKS), a commonly used weighted moving average. However, the weights of the Gaussian kernel are also multiplied by the weights mentioned above (Eq. (4)) to correct for the imbalanced data. The same weights are applied to the moving quantiles, which are calculated by linear interpolation from the empirical cumulative distribution function, as proposed by Parzen [36]. This way, the asymmetry and heteroscedasticity of the variance are disclosed without assuming its distribution. In the second method, the regression is obtained from support vector regression (SVR). Here, the scikit-learn package [37] is used to establish the regressions. To obtain non-parametric regressions, Gaussian (also called radial basis function) kernels were chosen.

The optimal hyperparameters (the kernel length scale σ of the GKS and the kernel coefficient γ and regularisation parameter C of the SVR) were found by means of a grid search, during which the average weighted sum of squares (Eq. (4)) from a five-fold cross-validation was minimised.

The fitted models and regression lines of the evacuation data and the routine data can then be compared to discuss the differences in traffic dynamics. One reason that might partly explain observed differences could be a change in the average vehicle lengths. Therefore, this method proposes to analyse the vehicle lengths as well. The lengths can be calculated as given in Eq. (5) [38,39]:

$$l = \frac{vo}{q} \tag{5}$$

where l is the arithmetic average length (m/veh) of all vehicles passing by the detector, v is the average speed (m/s), o is the detectors occupancy (–), which is the fraction of the sampling period for which a vehicle is present at the detector location, and q is the flow (veh/s) passing by the detector (all during the five-minute interval).

3. Traffic dynamics analyser

The methodology presented in Section 2 was implemented in a tool with a graphical user interface (see Fig. 2). This tool allows the user to extract PeMS data from different vehicle detection stations at different periods (scenarios) and to automate the analysis. The tool, called Traffic Data Analyser (TDA), is released in open access on Github and Zenodo [40]. What follows is a description of the different uses of the methodology for traffic evacuation data analysis using TDA.

The user must specify their PeMS account details, the identification number of the vehicle detector stations they intend to analyse, as well as the timespans they are interested in. The TDA is then able to log into the platform and automatically extract all required data. Hereafter, it processes the data by executing the necessary conversions and calculates the traffic density and the average vehicle lengths. If the user has used TDA before, they can also use the spreadsheet that they generated before, rather than downloading and processing all data again. Next, TDA generates the graphs as requested by the user.

Since our proposed methodology advises the user to visually inspect the relationships between the fundamental variables, the tool has been developed to generate graphs for each detector station individually. Speed, flow, and densities can be plotted for each lane of these stations, both as time series and as scatterplots. These graphs are valuable to perform a visual inspection of the data.

Moreover, TDA can aggregate the speed, flow, and density data on the scenario-level (evacuation versus routine) and provide the scatterplots. It also allows fitting (predefined or user-defined) models in accordance with our proposed methodology (see Section 2.4). In addition to the graphs, a second spreadsheet is created that contains the values of the fitted parameters, as well as the confidence intervals of these values. Examples of these graphs and tables are shown in Section 4.

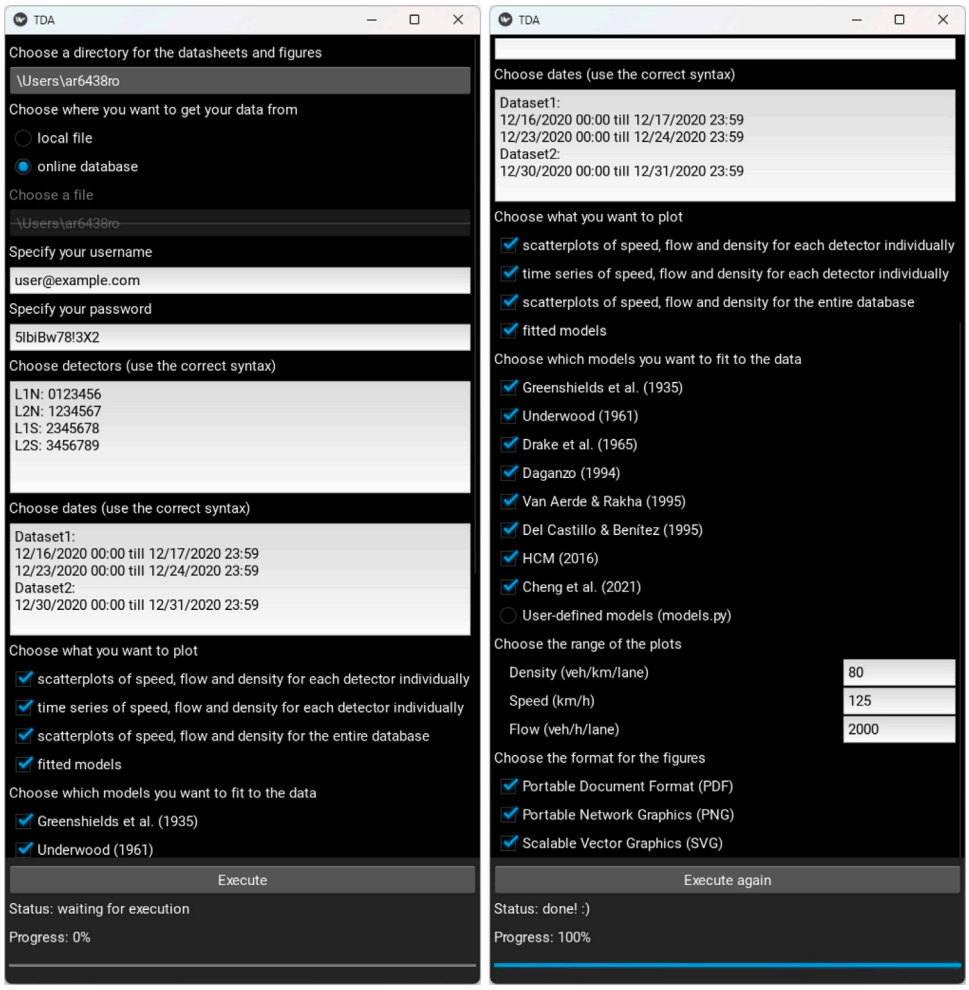

Fig. 2. Graphical user interface of the traffic data analyser.

4. The 2020 Glass Fire case study

In this section, we demonstrate the methodology through a case study: the 2020 Glass Fire. The Glass Fire was chosen as it led to a large-scale evacuation. Moreover, US 101, which is adjacent to the evacuation zone, is equipped with dual loop detectors, allowing for the measurement of flow, speed, and occupancy at the time of the evacuation. This section provides a brief overview of the event, followed by a presentation of the data selection process. This section ends with an analysis of the traffic dynamics on US 101 during the routine scenario (before the fire event) and the evacuation scenario (during the fire event). The goal is to identify if similar trends are found in the 2020 Glass Fire as were found in the Kincade Fire [19] as well as previous hurricane events [18].

4.1. Overview of the fire event

The 2020 Glass Fire started on 27 September 2020 just before 4 am and continued burning for 24 days until it was fully contained (on 20 October 2020) [41]. The ignition point was located in Napa County, California, United States, but the fire expanded rapidly to Sonoma County, due to the extremely high temperatures, strong winds and unprecedented drought [42]. By the second day, approximately 14 700 hectares (36 400 acres) of land has been affected, which is more than half of the eventually affected area (27 300 hectares or 67 500 acres) [41]. The ignition point and eventual perimeter of the fire are displayed in Fig. 3. On the second day, the fire reached the towns of Santa Rosa, Calistoga, and Saint Helena. In total, 1555 structures were destroyed [41] (of which 42% were residential) and 282 structures were damaged (of which 57% were residential),[1] making this fire the tenth most destructive wildfire in California to date [43].

Both Sonoma County and Napa County are divided into zones to manage evacuations during emergencies. In Sonoma County, all evacuation orders were issued on the 27th and the 28th of September [44], while in Napa, the last order was issued on the 4th of October. All orders were lifted between the 2nd and the 19th of October.[2] The evacuation zones for which a warning or order were issued, are shown in Fig. 3.

4.2. Data selection for the fire event

Only one route in the vicinity of the evacuation zones is equipped with vehicle detection stations (VDSs): the federal highway US 101. This highway runs straight through Sonoma County and it is the only route with multiple lanes in each direction and grade-separated junctions. It has a speed limit of 65 mi/h (≈105 km/h).

There are 301 vehicle detection stations along which congestion occurs in Sonoma County. All were considered in the selection process presented in Section 2.3. The outcome is summarised in the flowchart in Fig. 4. Eventually, fifteen stations were discarded after the visual inspection. For seven of these stations, detectors were present on an

[1] Glass Fire Incident Update, posted on Twitter by CAL FIRE.
[2] News updates, posted online by ABC7 News.

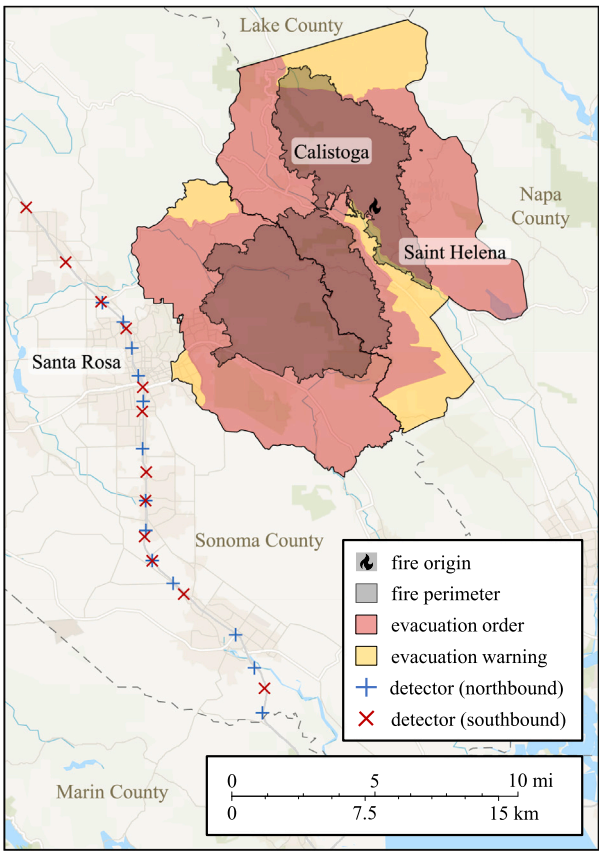

Fig. 3. Map (ESRI) of the wildfire incident. The evacuation warnings and orders for both Sonoma [44] and Napa (News updates, posted online by Bay City News) are coloured yellow and red respectively. The ignition point is marked with a flame symbol and the final perimeter of the fire is drawn in black [41]. (For interpretation of the references to colour in this figure legend, the reader is referred to the web version of this article.)

Table 1
Time periods of data extraction (day/month) and the corresponding flow.

Scenario	Start	End	Week	Traffic flow (veh/day)
Routine	08/31	09/02	36	22 399
	09/14	09/16	38	22 140
	09/21	09/23	39	22 690
Evacuation	09/28	09/30	40	22 295

on-ramp, an off-ramp, or a weaving zone, despite them being labelled as "mainline" in the PeMS database. The other eight discarded stations had one or more detectors that produced unreliable data. The final selection of VDSs is presented in Fig. 3.

The first evacuation orders were issued on Sunday the 27th of September. After analysing the traffic flow, it was decided to consider an evacuation scenario that starts on Monday the 28th and ends on Wednesday the 30th of September (Week 40). The reason for this decision is explained in more detail in Section 4.3. To compare the data with normal traffic, routine data is extracted one week earlier (Week 39), two weeks earlier (Week 38), and four weeks earlier (Week 36), from Monday to Wednesday as well. The reason why Week 37 is not included is because of Labor Day, on Monday the 7th of September. This day, traffic flow is significantly different and traffic dynamics are also considered to differ (as "weekend"-dynamics are expected). Table 1 summarises the time periods of data extraction. The average flow during these periods is also shown.

PeMS also provides incident reports. In this case, most of the incidents are vehicles or objects that briefly obstruct the road. None of the incidents led to lane closures or influenced the traffic dynamics considerably. A complete list of incidents is provided in [28].

4.3. Analysis of the traffic dynamics

We have extracted, processed and published the data in open access [45]. This section analyses the data.

Fig. 5 shows the hourly flow and speed of the traffic on US 101 before and during the evacuation. The flows and speeds are obtained by averaging the values of all twenty-five selected detectors. Curves of the different weeks are overlaid to demonstrate the recurring trends. The earliest week is Week 34, on which the new school year started. It can be easily noticed that the routine traffic flows are regular, as all blue curves overlap well. The one exception is Monday the 7th of September 2020 (Week 37), as it is a national holiday (*Labor Day*).

The fire stared early on Sunday the 27th of September (Week 40). Apart from relatively small evacuation orders at a distance equal to 25 km from US 101, no orders are issued until late in the evening [41]. The effect of the wildfire on the traffic flow is clearly visible during the last two hours. However, during these two hours, the traffic flow is rather low (i.e., no densities beyond 25 veh/km/lane are recorded). It was therefore decided to consider the start of the evacuation scenario on Monday (see Table 1) and end on Wednesday. This also eliminates the effect of the weekend on the traffic dynamics.

Fig. 6 shows the scatterplot of the extracted data. Clearly, congestion occurs during the evacuation (as well as during routine conditions). However, most of the data points have a low traffic density (98.6% of all points have a density below 20 veh/km/lane). This confirms the need for weighting when fitting the speed-density relationship to the data (see Section 2.4).

To apply our suggested methodology, the models by Daganzo, Van Aerde and Rakha, and Cheng et al. are fitted to the data using the TDA. The results are presented graphically in Fig. 6 and numerically in Table 2. The table shows the optimal model parameters, the confidence margins and the ratios φ, which represent the value of the parameter during the evacuation scenario, relative to the value during the routine scenario.

The trends of the data can also be presented without assuming a relationship between speed and density. Fig. 7 presents the weighted moving average achieved by Gaussian kernel smoothing (GKS). A kernel length scale σ of 2.750 veh/km/lane was used. The coloured lines represent the average values and the coloured surfaces are bounded by the 5 to 95 percentiles. Fig. 7 also shows the lines obtained with support vector regression (SVR). The kernel coefficient γ and the regularisation parameter C are 60 and 0.028 respectively for the evacuation scenario and 94 and 0.024 for the routine scenario.

Fig. 7 shows slight differences between the two scenarios. Comparing evacuation and routine scenarios, the average speed reduction for densities between 0 and 60 veh/km/lane equals 1.07 km/h for GKS and 1.23 km/h for SVR. The capacity reduces by 1.9% (GKS) or 3.1% (SVR). The parametric model fits show small differences between the scenarios as well (see Fig. 6 and Table 2).

Fig. 8 visualises the sample distribution of average vehicle lengths for the evacuation scenario and the routine scenario. Both the histogram and the cumulative probability curve are constructed by weighting the average vehicle lengths with the flow of the interval and lane in question to obtain car-based distributions. The histograms of both scenarios show a substantial overlap of 96.0%, suggesting a minimal disparity in the distributions of vehicle lengths.

5. Discussion

Overall, the methodology and accompanying TDA tool were used to collect and analyse traffic data before and after the 2020 Glass Fire in Sonoma County, California. The process allows the user to input the detector stations as well as the dates of the different scenarios and

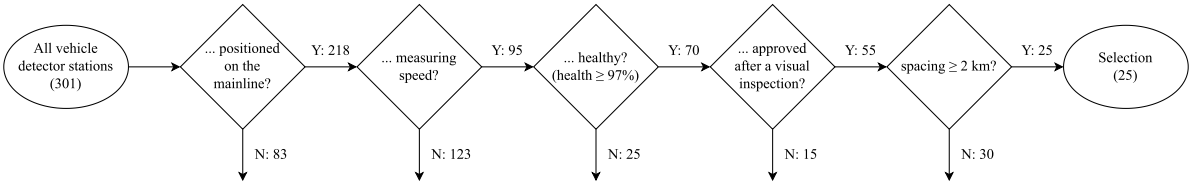

Fig. 4. Flowchart of the selection process for the vehicle detection stations for our case study.

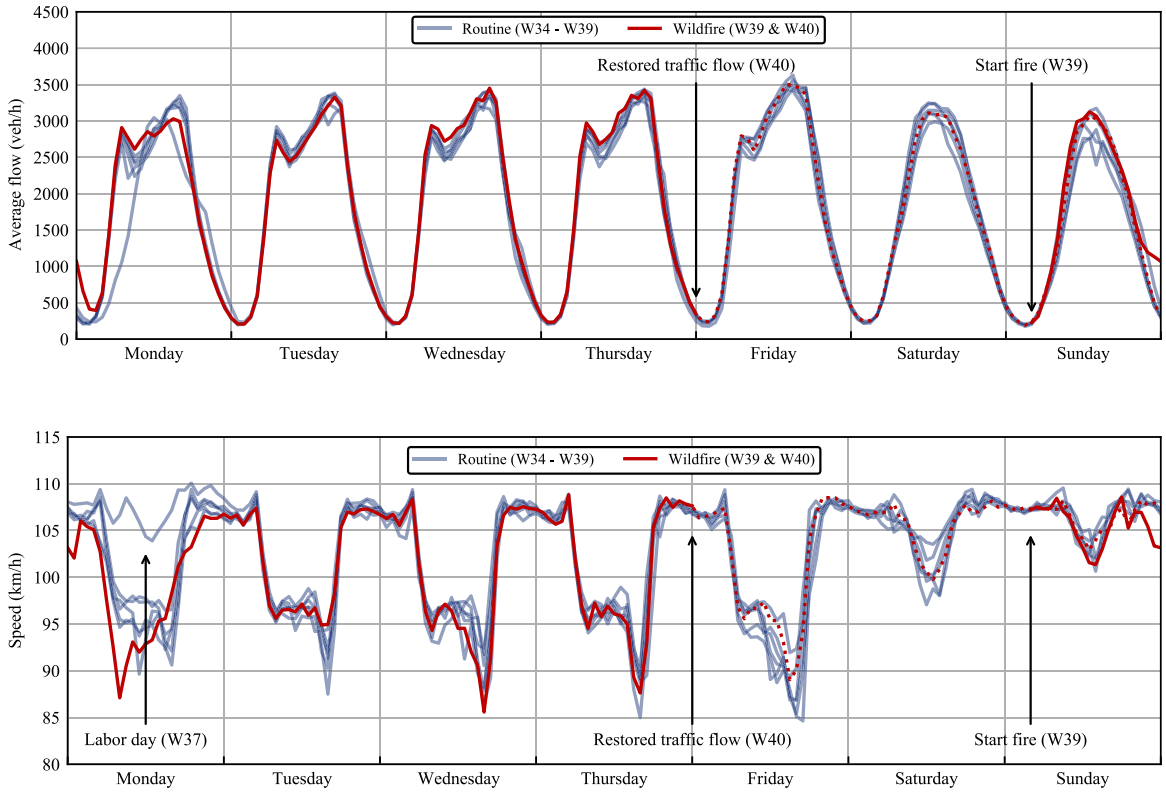

Fig. 5. Hourly flow and speed, averaged over all detectors, before and during the wildfire. (For interpretation of the references to colour in this figure legend, the reader is referred to the web version of this article.)

Table 2
Best fit values and confidence margin of the model parameters.

Model	Parameters	Best fit ± 95% confidence margin				φ (%)
		Routine		Evacuation		
Daganzo [23]	v_f (km/h)	102.1	±0.12	101.7	±0.21	99.6
	k_c (veh/km/lane)	14.1	±0.03	13.6	±0.05	96.3
	k_j (veh/km/lane)	192.2	±2.14	230.8	±7.58	120.1
	WRMSE (km/h)	6.19		6.98		
Van Aerde & Rakha [24]	v_f (km/h)	105.8	±0.17	105.0	±0.29	99.2
	a (km lane/veh)	4.58E−03	±6.9E−05	4.16E−03	±1.5E−04	90.7
	b (km^2 lane/veh/h)	1.59E−01	±7.7E−03	1.29E−01	±1.3E−02	81.0
	c (h lane/veh)	5.83E−04	±3.0E−06	6.25E−04	±6.3E−06	107.3
	WRMSE (km/h)	5.96		6.77		
Cheng et al. [27]	v_f (km/h)	109.2	±0.19	109.0	±0.34	99.8
	k_c (veh/km/lane)	24.5	±0.06	24.0	±0.12	97.6
	m (–)	2.27	±0.01	2.25	±0.03	99.2
	WRMSE (km/h)	6.36		7.32		

obtain the spreadsheet and the graphs for each station (individually and collectively) to better understand traffic dynamics of evacuation scenarios and routine scenarios on highways in the state of California. As the TDA is released in open access, the tool and its accompanying methodology are presented here to promote its use. With TDA, past and future fires in California can be analysed in a similar way to better understand traffic dynamics in different types of fires, communities, highways, and evacuation scenarios. It is hoped that the methodology presented can be applied to other traffic databases around the world. The use of the TDA allows for a comprehensive understanding of the potential change in speed, flow, and occupancy on highways during emergency events, such that existing traffic models can be updated

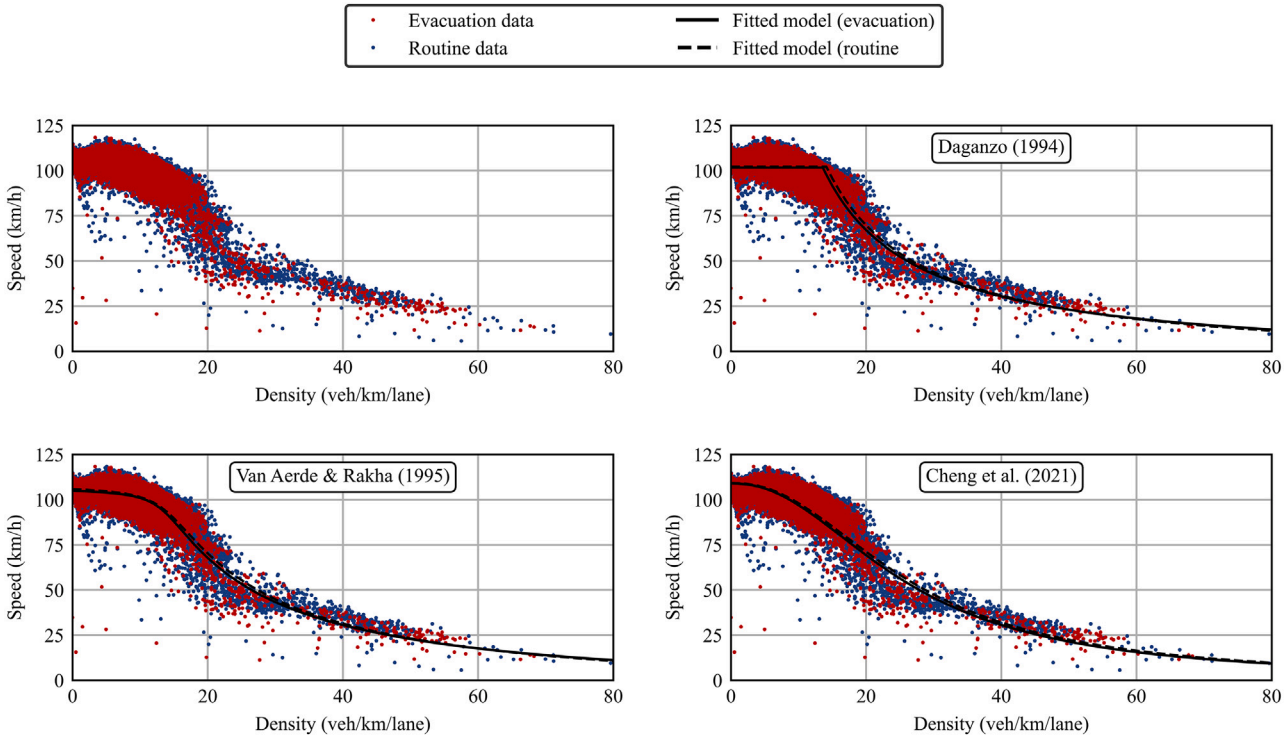

Fig. 6. Speed-density data and the fitted models for the evacuation data and the routine data. (For interpretation of the references to colour in this figure legend, the reader is referred to the web version of this article.)

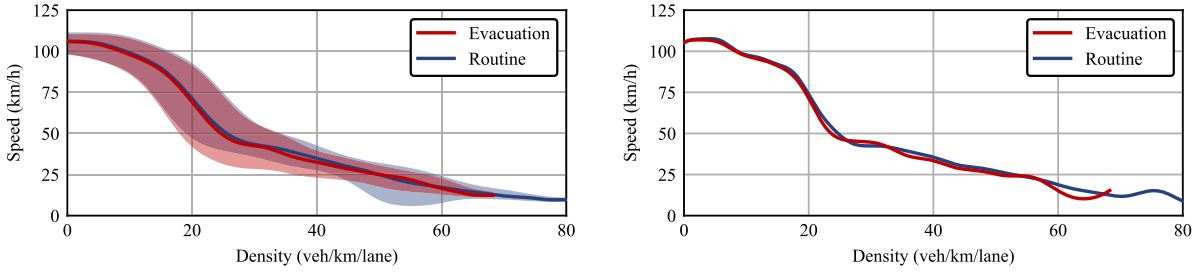

Fig. 7. Non-parametric regression, obtained by GKS (left) and SVR (right). (For interpretation of the references to colour in this figure legend, the reader is referred to the web version of this article.)

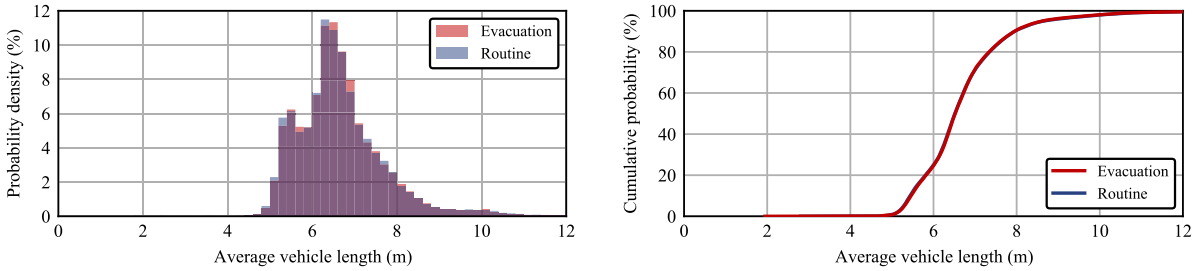

Fig. 8. Probability density and cumulative probability of the average vehicle length. (For interpretation of the references to colour in this figure legend, the reader is referred to the web version of this article.)

to account for evacuation scenarios. In turn, these and future findings can be used to improve the way in which communities plan for wildfires before an event and emergency authorities make decisions about evacuation, including instituting traffic management solutions, in real-time.

The proposed methodology and TDA were then implemented in a case study focused on the 2020 Glass fire. Results from the TDA demonstrate an average reduction in speed of 1.25 km/h (GKS) to 1.72 km/h (SVR) when comparing evacuation scenarios with routine scenarios. The road capacity drops by 2.1% (GKS) to 4.7% (SVR). However, this difference was smaller than that identified by Rohaert et al. [19] in their study of the 2019 Kincade Fire (i.e., a study that also analysed movement along US 101). The difference between the Kincade Fire and the Glass Fire is likely related to the position of the fire and evacuation zones in relation to US 101. During the Kincade Fire, the affected evacuation zones surrounded both sides (i.e., east and west) of US 101; whereas in the Glass Fire, the highway was only in close

vicinity to the affected areas (on the east). Consequently, the proportion of background traffic is expected to be higher for the 2020 fire.

Also, previous studies of wildfire and hurricane events suggest that evacuees often choose to leave with larger-sized vehicles (e.g., boat trailers, caravans, campers, or vans) during evacuation [46,47]. This might (partially) explain the reduced road capacity when the flow is expressed in vehicles rather than passenger car equivalents. During the 2019 Kincade Fire, the distribution of vehicle lengths changed significantly, while this is not the case for the 2020 Glass Fire (see Fig. 8). Therefore, Fig. 8 substantiates the assumption that 'background traffic' was more dominant on US 101 during the Glass Fire evacuation, likely diluting the effect of evacuee movement on the traffic dynamics. This explains why the difference in speed between the two scenarios is small.

The results of this work indicate the need for dedicated calibration and validation efforts of traffic models used to predict the evacuation time during wildfires. The distance of the fire location and evacuation zones from the impacted roads and highways is one of the factors influencing the results of traffic models. This finding also aligns with the results from the recent study by Hou et al. [48], which found that the impact on traffic performance reduces when the fire distance increases. The PeMS database collects traffic data from specific highways and freeways equipped with vehicle detection stations. It does not collect data from the other roads located closer to the fire region (e.g., collector or arterial roads). To compensate for this limitation with the PeMS database, other complementary datasets, such as GPS trajectory data [49], can help to measure traffic performance. Using complementary data sources can also improve the performance of the wildfire evacuation models.

As with any study, it is important to acknowledge the limitations associated with this work. One of them, in particular, is the fact that US 101 is further away from the affected area in the 2019 Glass Fire. Also, the PeMS database only collects traffic data from freeways, whereas in many cases the important traffic dynamics also occur on smaller roads. In this case, we only have traffic movement data on the main roads, rather than data from all the roads used for evacuation.

6. Conclusion

This paper presents a novel methodology for the analysis of traffic data in wildfire evacuation scenarios, based on both fitting parametric macroscopic traffic models and non-parametric machine learning regressions. The methodology has been implemented in a tool called Traffic Dynamics Analyser (TDA), which is made available for free for all interested parties [40] and has been demonstrated through a case study of the 2020 Glass Fire. The data from this case study has also been made available openly [45]. Results show the need for understanding traffic evacuation dynamics during wildfires and how this can be reflected in wildfire evacuation model development, calibration, and validation efforts.

Declaration of competing interest

The authors declare no conflict of interest associated with the manuscript.

Data availability

Data are publicly available

Acknowledgements

This work has been funded under award 60NANB21D118 from the National Institute of Standards and Technology (NIST), U.S. Department of Commerce. The authors would like to thank the WUI-NITY team (Jonathan Wahlqvist, Guillermo Rein, Harry Mitchell, Nikolaos Kalogeropoulos, Steve Gwynne, Hui Xie, Peter Thompson, Max Kinateder, Hamed Mozaffari Maaref, Maxine Berthiaume, Noureddine Bénichou, and Amanda Kimball). We also acknowledge the technical panel of the project for their support and guidance: Carole Adam, Amy Christianson, Tom Cova, Lauren Folk, Abishek Gaur, Paolo Intini, Justice Jones, Bryan Klein, Chris Lautenberger, Ruggiero Lovreglio, Jerry McAdams, Ruddy Mell, Elise Miller-Hooks, Cathy Stephens, Steve Taylor, Sandra Vaiciulyte, Xilei Zhao, Rita Fahy, Lucian Deaton, and Michele Steinberg.

References

[1] J.G. Pausas, J.E. Keeley, Wildfires and global change, Front. Ecol. Environ. 19 (7) (2021) 387–395.
[2] A. Bento-Gonçalves, A. Vieira, Wildfires in the wildland-urban interface: Key concepts and evaluation methodologies, Sci. Total Environ. 707 (2020) 135592.
[3] E. Ronchi, S.M. Gwynne, G. Rein, R. Wadhwani, P. Intini, A. Bergstedt, e-Sanctuary: Open Multi-Physics Framework for Modelling Wildfire Urban Evacuation, Fire Protection Research Foundation Quincy, 2017.
[4] E. Ronchi, S.M. Gwynne, G. Rein, P. Intini, R. Wadhwani, An open multi-physics framework for modelling wildland-urban interface fire evacuations, Saf. Sci. 118 (2019) 868–880.
[5] P.E. Dennison, T.J. Cova, M.A. Mortiz, WUIVAC: a wildland-urban interface evacuation trigger model applied in strategic wildfire scenarios, Nat. Hazards 41 (1) (2007) 181–199.
[6] A. Veeraswamy, E.R. Galea, L. Filippidis, P.J. Lawrence, S. Haasanen, R.J. Gazzard, T.E. Smith, The simulation of urban-scale evacuation scenarios with application to the Swinley forest fire, Saf. Sci. 102 (2018) 178–193.
[7] J. Wahlqvist, E. Ronchi, S.M. Gwynne, M. Kinateder, G. Rein, H. Mitchell, N. Bénichou, C. Ma, A. Kimball, E. Kuligowski, The simulation of wildland-urban interface fire evacuation: The WUI-NITY platform, Saf. Sci. 136 (2021) 105145.
[8] S. Grajdura, S. Borjigin, D. Niemeier, Fast-moving dire wildfire evacuation simulation, Transp. Res. D 104 (2022) 103190.
[9] S.D. Wong, J.C. Broader, J.L. Walker, S.A. Shaheen, Understanding California wildfire evacuee behavior and joint choice making, Transportation (2022).
[10] H. Mitchell, S. Gwynne, E. Ronchi, N. Kalogeropoulos, G. Rein, Integrating wildfire spread and evacuation times to design safe triggers: Application to two rural communities using PERIL model, Saf. Sci. 157 (2023) 105914.
[11] D. Singh, P. Ashton, T. Dess, M. Harper, E. Kuligowski, P. Gamage, L. Marquez, V. Lemiale, J. Halliday, R. McKenzie, M. Prakash, Bushfire evacuation decision support system use in incident management training, Aust. J. Emerg. Manage. 37 (4) (2022) 73–76.
[12] E. Kuligowski, Evacuation decision-making and behavior in wildfires: Past research, current challenges and a future research agenda, Fire Saf. J. 120 (2021) 103129.
[13] E. Ronchi, S. Gwynne, Computational evacuation modeling in wildfires, in: S.L. Manzello (Ed.), Encyclopedia of Wildfires and Wildland-Urban Interface (WUI) Fires, Springer International Publishing, Cham, 2019, pp. 1–10.
[14] P. Intini, E. Ronchi, S. Gwynne, A. Pel, Traffic modeling for wildland–urban interface fire evacuation, J. Transp. Eng. A 145 (3) (2019) 04019002.
[15] N. Wetterberg, E. Ronchi, J. Wahlqvist, Individual driving behaviour in wildfire smoke, Fire Technol. 57 (3) (2021) 1041–1061.
[16] B. Zhao, S.D. Wong, Developing transportation response strategies for wildfire evacuations via an empirically supported traffic simulation of Berkeley, California, Transportation Research Record: Journal of the Transportation Research Board 2675 (12) (2021) 557–582.
[17] X. Zhao, R. Lovreglio, E. Kuligowski, D. Nilsson, Using artificial intelligence for safe and effective wildfire evacuations, Fire Technol. 57 (2) (2021) 483–485.
[18] V. Dixit, B. Wolshon, Evacuation traffic dynamics, Transp. Res. C 49 (2014) 114–125.
[19] A. Rohaert, E.D. Kuligowski, A. Ardinge, J. Wahlqvist, S.M. Gwynne, A. Kimball, N. Bénichou, E. Ronchi, Traffic dynamics during the 2019 Kincade wildfire evacuation, Transp. Res. D 116 (2023) 103610.
[20] B. Greenshields, J. Bibbins, W. Channing, H. Miller, A study of traffic capacity, Highw. Res. Board Proc. 1935 (1935).
[21] R.T. Underwood, Speed, volume and density relationships, in: Quality and Theory of Traffic Flow. A Symposium, Yale University Bureau of Highway Traffic, Bureau of Highway Traffic, Yale University, 1961, pp. 141–188.
[22] J. Drake, J. Schofer, A. May, A statistical analysis of speed-density hypotheses, Traffic Flow Transp. (1965) 53–87.

[23] C.F. Daganzo, The cell transmission model: A dynamic representation of highway traffic consistent with the hydrodynamic theory, Transp. Res. B 28 (4) (1994) 269–287.
[24] M. Van Aerde, H. Rakha, Multivariate calibration of single regime speed-flow-density relationships, in: Pacific Rim TransTech Conference. Vehicle Navigation and Information Systems Conference Proceedings, sixth ed., IEEE, 1995, pp. 334–341.
[25] N. Wu, H. Rakha, Derivation of van aerde traffic stream model from tandem-queuing theory, Transp. Res. Record: J. Transp. Res. Board 2124 (1) (2009) 18–27.
[26] J.M. Del Castillo, F.G. Benítez, On the functional form of the speed-density relationship - Part I: General theory, Transp. Res. B 29 (5) (1995) 373–389, Publisher: Pergamon.
[27] Q. Cheng, Z. Liu, Y. Lin, X.S. Zhou, An s-shaped three-parameter (S3) traffic stream model with consistent car following relationship, Transp. Res. B 153 (2021) 246–271.
[28] E. Ronchi, J. Wahlqvist, A. Rohaert, E.D. Kuligowski, N. Janfeshan Araghi, G. Rein, H. Mitchell, N. Kalogeropoulos, M. Kinateder, H.M. Maaref, M. Berthiaume, A. Kimball, WUI-NITY3: Multi-Method Traffic Movement Data Collection for WUI Fire Evacuation Modelling, Tech. Rep., Fire Protection Research Foundation, Quincy, MA (USA), 2023, p. 80.
[29] C.D. of Transportation, PeMS User Guide, California Department of Transportation, 2020.
[30] D.L. Woods, B.P. Cronin, R.A. Hamm, Speed Measurement with Inductance Loop Speed Traps, Tech. Rep. FHW A/TX-95/1392-8, Texas Transportation Institute, Austin, 1994, p. 78.
[31] L.A. Klein, M.R. Kelly, Detection Technology for IVHS, Volume 1, Tech. Rep. FHWA-RD-95-100, US Department of Transportation, Federal Highway Administration, Washington, DC, 1996.
[32] M.D. of Transportation, Evaluation of Non-Intrusive Technologies for Traffic Detection, Tech. Rep. NIT Phase II Report 3683, Minnesota Department of Transportation, 2002.
[33] K. Levenberg, A method for the solution of certain non-linear problems in least squares, Quart. Appl. Math. 2 (2) (1944) 164–168.
[34] D.W. Marquardt, An algorithm for least-squares estimation of nonlinear parameters, J. Soc. Ind. Appl. Math. 11 (2) (1963) 431–441.
[35] X. Qu, S. Wang, J. Zhang, On the fundamental diagram for freeway traffic: A novel calibration approach for single-regime models, Transp. Res. B 73 (2015) 91–102.
[36] E. Parzen, Nonparametric statistical data modeling, J. Amer. Statist. Assoc. 74 (365) (1979) 105–121.
[37] F. Pedregosa, G. Varoquaux, A. Gramfort, V. Michel, B. Thirion, O. Grisel, M. Blondel, P. Prettenhofer, R. Weiss, V. Dubourg, J. Vanderplas, A. Passos, D. Cournapeau, M. Brucher, M. Perrot, E. Duchesnay, Scikit-learn: Machine learning in python, J. Mach. Learn. Res. 12 (2011) 2825–2830.
[38] C. Chen, Freeway Performance Measurement System (PeMS), Institute of Transportation Studies, University of California, 2003.
[39] D.J. Dailey, A statistical algorithm for estimating speed from single loop volume and occupancy measurements, Transp. Res. B 33 (5) (1999) 313–322.
[40] A. Rohaert, Traffic dynamics analyser (TDA), 2022, http://dx.doi.org/10.5281/zenodo.7181486.
[41] G.I. Morris, CAL FIRE 2020 Fire Siege, Tech. Rep., California Department of Forestry and Fire Protection, 2020.
[42] Glass Fire Natural Resources Update, Tech. Rep., California State Parks, Bay Area District Natural Resource Management Program, 2021.
[43] C.D. of Forestry, F. Protection, Top 20 Most Destructive California Wildfires, Tech. Rep., California Department of Forestry and Fire Protection, 2022.
[44] S.C. Emergency Management, Glass Fire Evacuation Orders History, Tech. Rep., Emergency Management, Sonoma County, 2020.
[45] A. Rohaert, N. Janfeshan Araghi, E.D. Kuligowski, E. Ronchi, Dataset of traffic dynamics during the 2020 glass wildfire evacuation, 2023, http://dx.doi.org/10.5281/zenodo.7483487, Version Number: 1, Type: dataset.
[46] P. Maghelal, X. Li, W.G. Peacock, Highway congestion during evacuation: examining the household's choice of number of vehicles to evacuate, Nat. Hazards 87 (3) (2017) 1399–1411.
[47] H.-C. Wu, M.K. Lindell, C.S. Prater, Logistics of hurricane evacuation in Hurricanes Katrina and Rita, Transp. Res. F 15 (4) (2012) 445–461.
[48] Z. Hou, J. Darr, M. Zhang, Predicting traffic performance during a wildfire using machine learning, Transp. Res. Record: J. Transp. Res. Board (2022) 036119812211265.
[49] X. Zhao, Y. Xu, R. Lovreglio, E. Kuligowski, D. Nilsson, T.J. Cova, A. Wu, X. Yan, Estimating wildfire evacuation decision and departure timing using large-scale GPS data, Transp. Res. D 107 (2022) 103277.